*Acta Oceanol. Sin.*, 2021, Vol. 40, No. 12, P. 27–38
https://doi.org/10.1007/s13131-021-1901-4
http://www.aosocean.com
E-mail: ocean2@hyxb.org.cn

# Source and magmatic evolution of ocean island basalts from the Pohnpei Island, Northwest Pacific Ocean: Insights from olivine geochemistry

Tong Zong[1], Zhenggang Li[2]*, Xuping Li[3], Yanhui Dong[2], Jihao Zhu[2]

[1] College of Architectural Engineering, Weifang University, Weifang 261061, China

[2] Key Laboratory of Submarine Geosciences, Second Institute of Oceanography, Ministry of Natural Resources, Hangzhou 310012, China

[3] Research Center of Continental Dynamics, College of Earth Science and Engineering, Shandong University of Science and Technology, Qingdao 266590, China

Received 23 April 2021; accepted 13 September 2021



**Abstract**

The compositional variability of ocean island basalts (OIBs) is thought to reflect partial melting of a lithologically-heterogeneous mantle source dominated by either pyroxenite or peridotite. The Pohnpei Island in Micronesia, which is associated with the Caroline hotspot, is suggested to have been generated from partial melting of a pyroxenite-rich mantle. To examine this hypothesis, we present new major- and trace-element compositions of olivine phenocrysts in basalts from the island. The olivines exhibit large systematic inter- and intra-crystalline compositional variability. In Sample DS1, olivines record compositional zonation, in which cores have relatively high Fo (77–85), Ni ($550\times10^{-6}$–$2\ 392\times10^{-6}$), and Fe/Mn ratios (66–82), whereas rims have lower Fo (71–78), Ni ($526\times10^{-6}$–$1\ 537\times10^{-6}$), and Fe/Mn ratios (51–62). By contrast, olivines within other samples preserve no clear compositional zonation, exhibiting similar or slightly lower Fo values (66–78), Ni contents ($401\times10^{-6}$–$1\ 268\times10^{-6}$), and Fe/Mn ratios (53–69) as the rims of zoned crystals. The distinct chemical contrast between the two different types of olivine suggests they formed in magma chambers at different depths. Analysis using forward petrological modeling and multi-element indicators (Fe/Mn, Zn/Fe, FC3MS ($FeO^T/CaO$–$(3\times MgO/SiO_2)$), Mn/Zn, and Ni/(Mg/Fe)) of whole-rock samples and high-Fo olivines is inconsistent with a pyroxenite-rich mantle source. We suggest these inconsistencies reflect an influence on the partition coefficients of Ni and Mn between olivine and liquid during melting at variable pressures and temperatures. In addition, magma recharge and mixing within the magmatic plumbing system can change the composition of olivine. We suggest that identification of the mantle source of OIBs in volcanic islands such as the Pohnpei Island using olivine geochemistry should be treated with caution.

**Key words:** olivine geochemistry, mantle source, magmatic evolution, ocean island basalt, Pohnpei Island

**Citation:** Zong Tong, Li Zhenggang, Li Xuping, Dong Yanhui, Zhu Jihao. 2021. Source and magmatic evolution of ocean island basalts from the Pohnpei Island, Northwest Pacific Ocean: Insights from olivine geochemistry. Acta Oceanologica Sinica, 40(12): 27–38, doi: 10.1007/s13131-021-1901-4

## 1 Introduction

It is widely believed that ocean island basalts (OIBs) are produced in deep-seated mantle plumes (Morgan, 1971). Mantle plumes are chemically and/or lithologically heterogeneous (Stracke, 2012; Huang and Zheng, 2017), and are interpreted to be triggered by mixing of recycled oceanic crust into the deep mantle (Hofmann and White, 1982; Rehkämper and Hofmann, 1997; Sobolev et al., 2007; Stracke, 2012). Entrained oceanic crust can react with mantle peridotite to form pyroxenite (Yaxley and Green, 1998; Wang et al., 2012; Herzberg et al., 2014; Heinonen and Fusswinkel, 2017), which melts preferentially relative to peridotite at the same pressure-temperature (*P*-*T*) conditions (Yaxley, 2000). Information concerning these processes can be preserved both in whole-rock samples of OIBs and the minerals they contain. In comparison with whole-rock compositions, which may be altered by processes such as fractional crystallization and magma mixing during ascent and storage (Shorttle, 2015; Lissenberg and MacLeod, 2016; O'Neill and Jenner, 2016; Paquet et al., 2016), minerals can more faithfully record chemical variations in the primary magmas as they are less easily reset during the processes that homogenize magmatic liquids (Putirka, 2008).

Olivine is the earliest crystallizing mineral at low pressures in almost all mantle-derived magmas and the most abundant mineral in the upper mantle (De Hoog et al., 2010; Ammannati et al., 2016; Zamboni et al., 2017; Shaikh et al., 2019). Comparisons between melt inclusions and host olivine grains that crystallized from primary melts have demonstrated they have similar patterns of incompatible trace element variability (Matzen et al., 2017a). As a consequence, olivine phenocrysts have been widely used to constrain the mantle source and magmatic evolution of basalts (Sobolev et al., 2005, 2007; De Hoog et al., 2010; Foley et

Foundation item: The Resources and Environment Projects of China Ocean Mineral R&D Association under contract No. DY135-E2-2-01; the Natural Science Foundation of Shandong Province under contract No. ZR2020QD076.
*Corresponding author, E-mail: lizg@sio.org.cn

al., 2013; De Maisonneuve et al., 2016; Herzberg et al., 2016; Collinet et al., 2017; Howarth and Harris, 2017; Li et al., 2020).

The Pohnpei Island in Micronesia is a volcanic island that is associated with the Caroline mantle plume (Dixon et al., 1984; Keating et al., 1984; Spengler et al., 1994; Courtillot et al., 2003; Jackson et al., 2017; Zhang et al., 2020a). Compared with typical mid-ocean ridge basalts (MORBs), elevated $^{3}He/^{4}He$ isotope ratios (7.6–12.8) in basalts from the Caroline Islands indicated a recycled oceanic crustal component within the Caroline mantle plume (Jackson et al., 2017). Zhang et al. (2020a) suggested that, based on the high Ni and low Ca and Mn contents of olivines, the Pohnpei lavas originated from a pyroxenite mantle source. However, many studies have found that partial melting (Niu et al., 2011; Putirka et al., 2018) and shallow crustal processing such as magma recharge and mixing (Gleeson and Gibson, 2019) can significantly impact the chemical compositions of olivines crystallized from peridotite-derived melts, such that they exhibit geochemical characteristics similar to olivines derived from pyroxenitic mantle (Sobolev et al., 2005, 2007; Niu et al., 2011; Matzen et al., 2017a, b; Putirka et al., 2018; Gleeson and Gibson, 2019). In this paper, we report high-precision major- and trace-element data from olivines in OIB-type basalts from the Pohnpei Island to constrain the mantle source of the basalts and their subsequent magmatic evolution. Using a comprehensive study of the chemical compositions of olivines and whole-rock samples, we find that widely-used multi-element indicators (Fe/Mn, Zn/Fe, Mn/Zn and Ni/(Mg/Fe)) for olivines yield contradictory results for the mantle lithology of the Pohnpei OIBs. Our results suggest that olivine geochemistry should be used with caution when attempting to discriminate the lithology of the mantle source of OIBs.

## 2 Geological background and previous study

The Pohnpei Island is the largest of three volcanic islands (Chuuk, Pohnpei and Kosrae) within the Caroline Islands (Fig. 1a), and are the products of hotspot-derived mantle magmatism (Mattey, 1982; Dixon et al., 1984; Keating et al., 1984; Jackson et al., 2017; Zhang et al., 2020a, b; Zong et al., 2020). The age and volume of magmatism decrease from the Chuuk Island to the Pohnpei Island to the Kosrae Island (Spengler et al., 1994), and there are no active hotspot volcanoes to the east of Kosrae (Zhang et al., 2020b). These observations indicate a gradual decline in magma production along the Caroline chain, and that activity related to the Caroline mantle plume has already ceased (Mattey, 1982; Zhang et al., 2020a, b).

The volcanic rocks erupted on the Pohnpei Island are alkaline and can be subdivided into shield-building lavas and post-shield deposits (Spengler, 1990). Spengler et al. (1994) further subdivided volcanism into three separate stages of activity, namely the main shield-building stage, the Awak volcanic series, and the Kupwuriso volcanic series. The isotopic compositions of the Pohnpei lavas indicate a hotspot origin, but Pb isotopes show that the three series did not originate from isotopically-homogeneous sources (Spengler et al., 1994). The five K-Ar ages between 0.9 Ma and 8.7 Ma reported by Dixon et al. (1984) overlap with those of Chuuk (14–4.3 Ma), but are inconsistent with a simple hotspot model. Rehman et al. (2013) suggested that the Caroline seamounts were formed by fracture-induced volcanism due to subduction-related tectonic activity. The $SiO_2$-undersaturated and $SiO_2$-saturated series were identified on the Pohnpei Island, they were argued to have originated from a compositionally homogenous mantle source, but formed under different temperatures and pressures (Zong et al., 2020). Compared with the Louisville seamount chains, the Pohnpei Island was formed by lower-degree mantle melting at greater depth, possibly because of the thicker lithosphere beneath the Pohnpei Island (Zong et al., 2020). Zhang et al. (2020a) proposed a two-stage model for the evolution of carbonated melts from the Pohnpei Island. The primary magmas of high-MgO (Stage 1) lavas are carbonated silicate melts that were de-carbonated and transformed into typ-

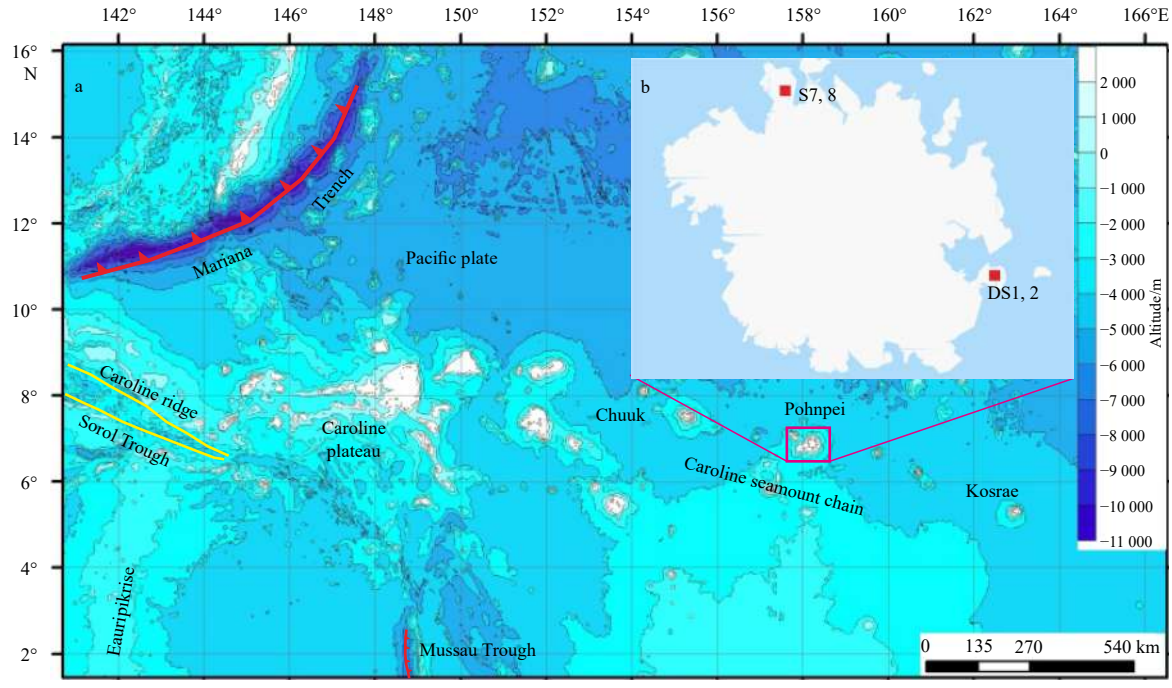


**Fig. 1.** Location and altitude map of the Pohnpei Island in the Pacific Ocean from Zong et al. (2020) (a) and map of the Pohnpei Island showing sample locations (b).

ical alkali OIBs in the deep lithospheric mantle. The high-MgO primary melts evolved towards low-MgO (Stage 2) melts, and underwent a closed-system evolution within the lithospheric plumbing system (Zhang et al., 2020a).

## 3 Samples and analytical methods

Olivines in nine thin sections from four basaltic samples (DS1, DS2, S7 and S8) were analyzed *in situ* to measure their major- and trace-element compositions. Samples DS1 and DS2, which were newly collected (Fig. 1b), have large phenocrysts (most are larger than 1 mm in diameter; Figs 2a and b). The phenocryst assemblages are composed mainly of euhedral and subhedral olivine (Figs 2c and d) and clinopyroxene. Olivines in Sample DS1 show compositional zonation, with large, homogeneous, unzoned cores and very thin rims apparent in backscattered electron images (Fig. 2e). The cores of zoned olivines are irregular to rounded in shape. The compositional zonation of olivines in Sample DS2 is less apparent than in DS1 (Fig. 2f). Olivines in Samples S7 and S8 show no compositional zoning (Zong et al., 2020), similar to those in Sample DS2. Whole-rock and olivine compositions of Samples S7 and S8 have been reported (Zong et al., 2020).

Both cores and rims of olivines in Sample DS1 were analyzed, whereas only olivine cores were measured in basalt Samples DS2, S7, and S8. The major-element compositions of olivines in Samples DS1 and DS2 were acquired using a JEOL JXA-8100 electron probe microanalyser (EPMA) at the Key Laboratory of Submarine Geosciences, Second Institute of Oceanography, State Oceanic Administration, Hangzhou, China. The instrument settings and analytical procedures follow Zong et al. (2020). Major and trace element analyses using laser-ablation inductively coupled plasma mass spectrometry (LA-ICP-MS) were performed in the Laboratory of Ocean Lithosphere and Mantle Dynamics (LOLMD) at the Institute of Oceanology, Chinese

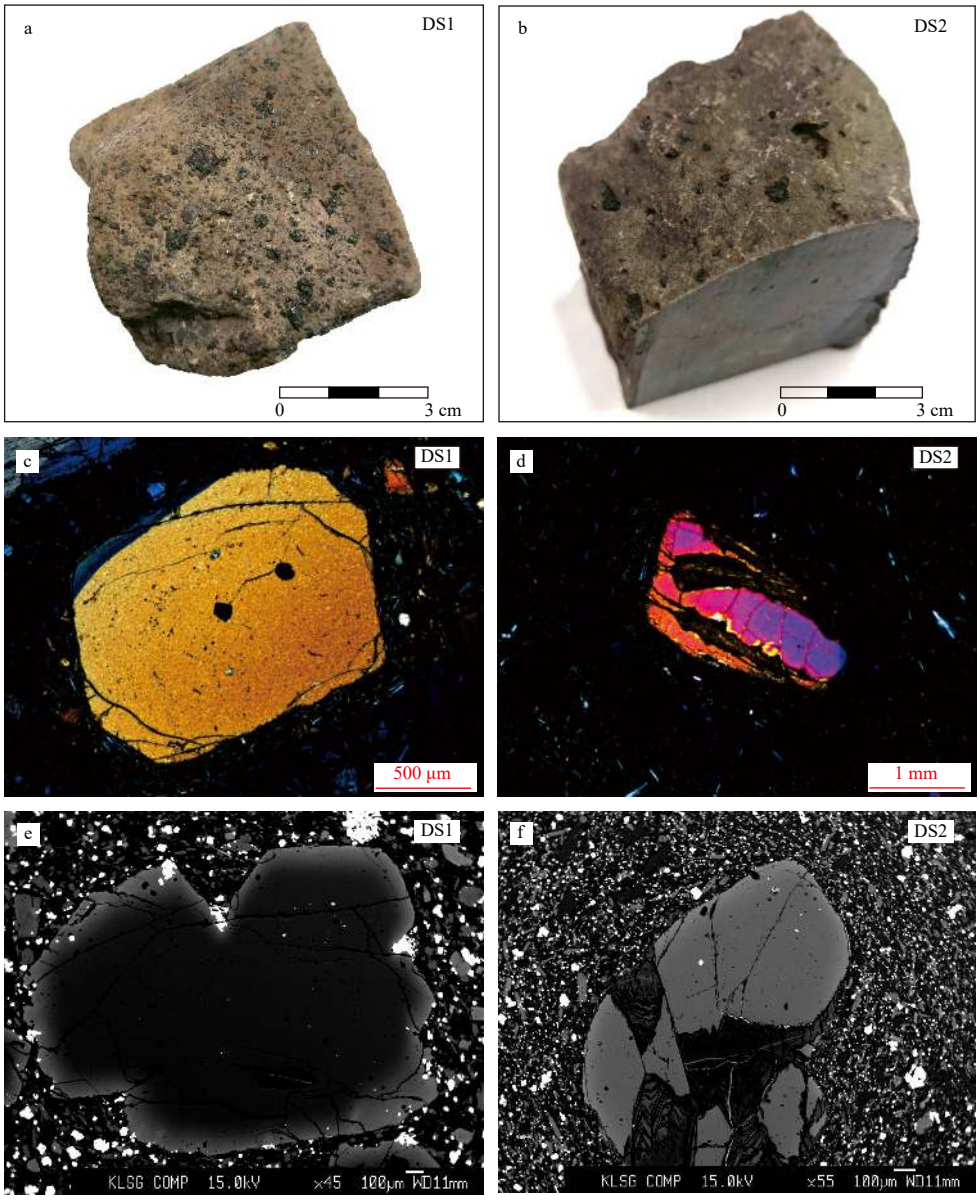


**Fig. 2.** Hand specimens (a, b), photomicrographs showing the textural characteristics of olivine (c, d), and back-scattered electron (BSE) (e, f) images of basalts from sample locations DS1 and DS2 on the Pohnpei Island.

Academy of Sciences, Beijing, China. A 193 nm ultra-short pulse excimer laser ablation system coupled with an Agilent 7900a ICP-MS instrument was used to acquire ion-signal intensities. Each spot analysis was conducted using a 40 μm spot and 3.62 J/cm$^2$ energy density with a repetition rate of 6 Hz. Acquisition times for each analysis were 25 s for background (gas blank) and 50 s for the unknown. USGS glasses (BCR-2G, BHVO-2G and BIR-1G) were used as external standards. Every eight unknown analyses were followed by analyses of standards GSE-1G and NIST SRM 610. The raw data were processed using the software ICPMS-DataCal (Liu et al., 2008), with $^{28}$Si as the internal standard for data calibration. Repeated data from standards GSE-1G, BCR-2G, BHVO-2G, and BIR-1G glasses are listed in Supplementary Table S1. The results obtained by LA-ICP-MS are consistent with EPMA results in terms of trace elements within the same olivine grain (Fig. A1 in Appendix). Whole-rock major- and trace-element analysis of Samples DS1 and DS2 followed the procedures of Zong et al. (2020).

## 4 Results

### 4.1 *Whole-rock major and trace elements*

The whole-rock major- and trace-element data from basalt samples DS1 and DS2 are listed in Supplementary Table S1. These samples have strikingly similar major oxide compositions but more variable trace element contents; Sample DS2 has higher trace element concentrations overall than Sample DS1 (Fig. 3; Fig. A2 in Appendix). The DS1 and DS2 basalts have higher MgO, FeO$^T$, MnO, and CaO contents than Samples S7 and S8, the latter of which have very similar major oxide and trace element contents (Fig. 3; Fig. A2 in Appendix). The chemical compositions of Samples DS1 and DS2 overlap with previously published data for the Pohnpei basalts (Mattey, 1982; Dixon et al., 1984; Jackson et al., 2017; Zhang et al., 2020a; Zong et al., 2020), and are similar to Stage 2 basalts reported by Zhang et al. (2020a) (Fig. 3; Fig. A2 in Appendix).

### 4.2 *In situ olivine major and trace elements*

The EMPA and LA-ICP-MS major- and trace-element data from olivines are listed in Supplementary Table S1. All olivines have CaO contents of higher than 0.10 wt.% (0.17–0.46 wt.%), indicating a magmatic origin (Thompson and Gibson, 2000; Ren et al., 2004). The Ca, Ni, and Mn contents and Fe/Mn ratios are similar to those in Pohnpei olivines reported by Zong et al. (2020) and Zhang et al. (2020a) at given Fo values (Fo = 100 × molar MgO/(MgO + FeO$^T$)) (Fig. 4).

Olivines in the studied samples exhibit large systematic inter-

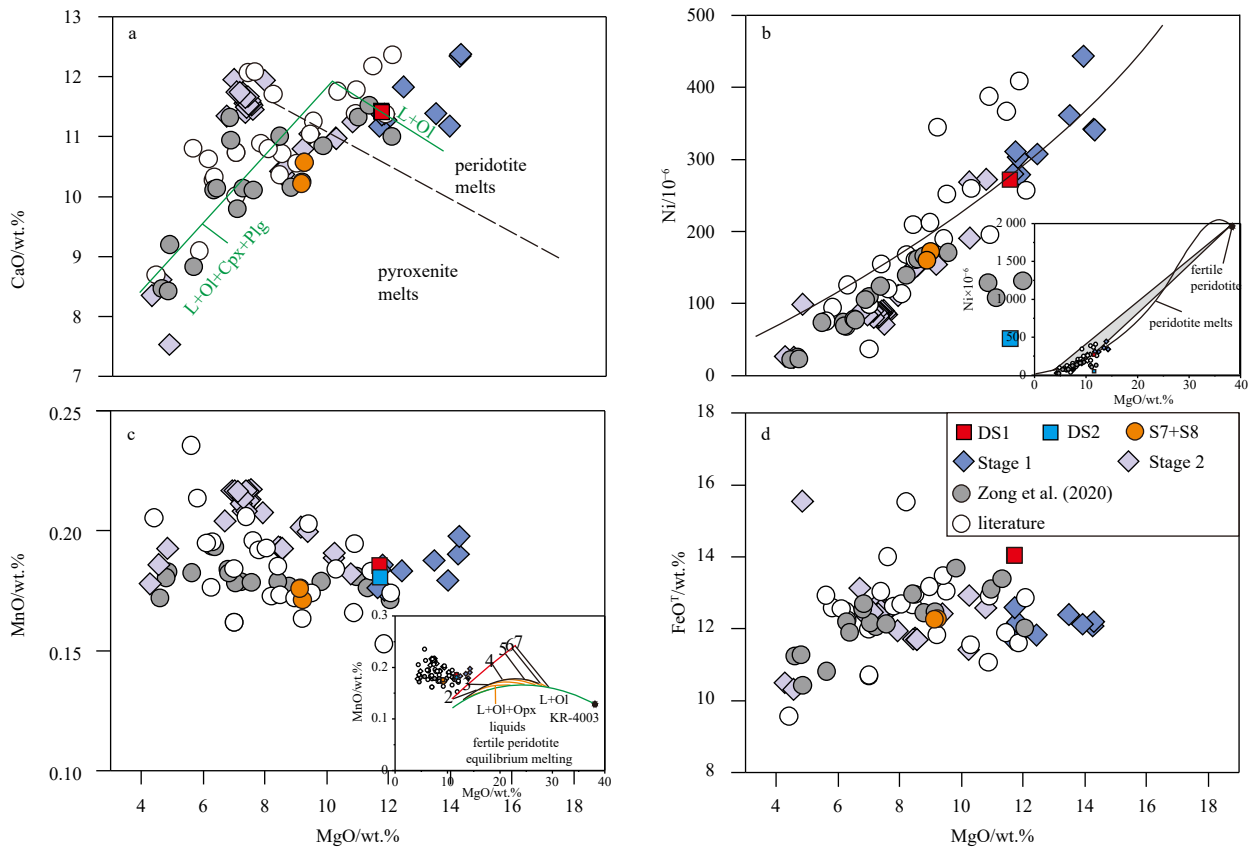


**Fig. 3.** CaO (a), Ni (b), MnO (c), and FeO$^T$ (d) contents plotted against MgO contents of basalts from the Pohnpei Island. Literature data are from Mattey (1982), Dixon et al. (1984), and Jackson et al. (2017), and Stage 1 and Stage 2 basalts are from Zhang et al. (2020a). a. The broken black line representing the boundary separating peridotite- and pyroxenite-derived primary magmas is from Herzberg and Asimow (2008). The green line represents the liquid line of descent formed by crystallization of olivine, then olivine (Ol) + clinopyroxene (Cpx) + plagioclase (Plg), following Herzberg and Asimow (2008). b. The black line represents the calculated Ni contents for partial melts of fertile peridotite formed by accumulated fractional melting. The insets in b and c followed Herzberg (2011). c. The MnO contents of experimental melts from peridotite KR-4003 (Walter, 1998) are shown in the inset, and the numbers 2 to 7 are pressures (10$^8$ Pa).

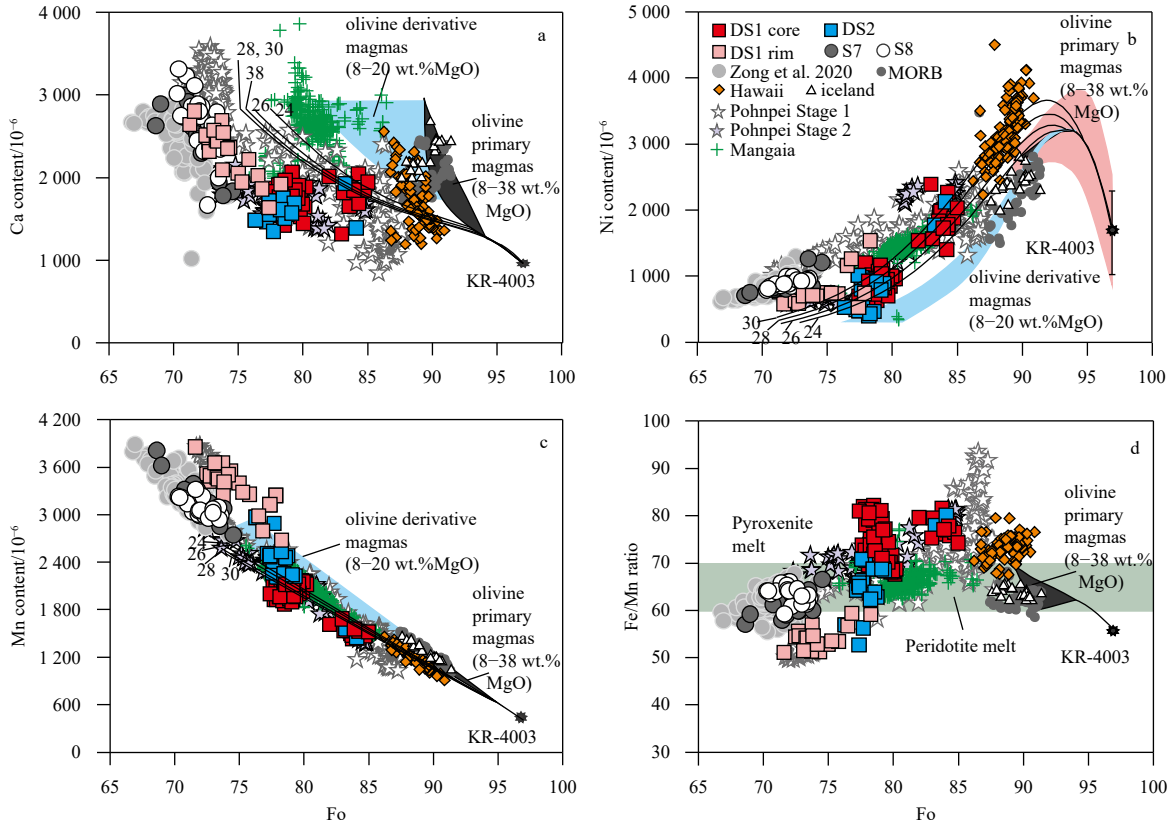


**Fig. 4.** Variations of Ca (a), Ni (b), Mn (c) contents and Fe/Mn ratios (d) against Fo values of olivines in the Pohnpei basalts. The data of Pohnpei olivines analyzed by Zong et al. (2020) and reported by Zhang et al. (2020a) for Stage 1 and Stage 2 basalts are also shown. Olivine data for MORB and Hawaiian and Icelandic basalts are from Sobolev et al. (2007). Black fields represent the calculated Ca, Ni, Mn, and Fe/Mn ratios in olivines crystallizing from primary melts derived from a fertile peridotite source, and contain 1 964 $\times 10^{-6}$ Ni, 3.45 wt.% CaO, and 0.13 wt.% MnO (Herzberg, 2011), the pink field represents the 1σ uncertainty for Ni (Herzberg et al., 2013). Light blue fields represent calculated olivine compositions from olivine-fractionated derivative liquids with 8–20 wt.% MgO. The assumed primary magma was that produced in experiment 40.06 by Walter (1998) on fertile peridotite KR-4003. Numbered black lines are for olivines modeled from olivine-fractionated derivative liquids with 20–38 wt.% MgO.

and intra-crystalline geochemical variations (Fig. 4; Fig. A3 in Appendix). Olivines in Sample DS1 show compositional zonation, in which cores have higher Fo (77–85) and Ni (550×$10^{-6}$–2 392×$10^{-6}$) and lower Mn (1 433×$10^{-6}$–2 393 ×$10^{-6}$) contents, and rims have lower Fo (71–78) and Ni (526×$10^{-6}$–1 537 ×$10^{-6}$) and higher Mn (2 681×$10^{-6}$–3 957 ×$10^{-6}$) contents. Calcium contents are nearly constant in cores, but increase gradually with decreasing Fo values in rims. Olivines in Sample DS2 have relatively low Fo (76–78), Ni (401×$10^{-6}$–1 014 ×$10^{-6}$), and Mn (2 215×$10^{-6}$–3 129× $10^{-6}$) contents. Olivines in Samples S7 and S8 have similar concentrations of Fo (66–75), Ni (711×$10^{-6}$–1 268 ×$10^{-6}$), and Mn (2 744× $10^{-6}$–3 813 ×$10^{-6}$), and concentrations of Ca that increase with decreasing Fo values.

The Fe/Mn ratios in the Pohnpei olivines are highly variable. In Sample DS1, olivine cores are characterized by the highest Fe/Mn ratios (66–82), whereas rims have the lowest ratios (51–62). Overall, Fe/Mn ratios in olivines from the studied samples, along with those reported by Zong et al. (2020) and Zhang et al. (2020a), are positively correlated against Fo values. The Ca/Fe ratios in olivines form a crescent-shaped trend against Fo values, whereas Ni/(Mg/Fe), Mn/Zn and Zn/Fe ratios show no systematic variation with Fo values (Fig. A4 in Appendix). The Ni/(Mg/Fe) ratios in the Pohnpei olivines display wide variability, even at high Fo values, and encompass the range of compositions shown by olivines in Hawaiian basalts and MORB.

## 5 Discussion

### 5.1 *Comparison of observed compositions with liquid lines of descent (LLDs)*

The chemical compositions of olivine with Fo greater than 90 can be used to infer the mantle source from which the basalts in which they occur were derived (Sobolev et al., 2007; Herzberg et al., 2014). However, it becomes a challenge when the olivine phenocrysts have Fo values of lower than 90, as fractional crystallization plays a significant role on olivine compositions (Herzberg et al., 2014, 2016). The studied olivines have Fo ranging from 66 to 85 (Fig. 3), and the presence of olivine and clinopyroxene phenocrysts in Samples DS1 and DS2 (Figs 2a and b) indicate that the primary magmas experienced fractional crystallization involving these two minerals. Crystallization of clinopyroxene will lead the derivative magma to be enriched in Ni and depleted in Ca and Mn, which will be reflected in the compositions of olivine crystallized from such magmas (Herzberg et al., 2013; Vidito et al., 2013), the olivines may be confused with those derived from pyroxenite sources (Herzberg et al., 2014). Consequently, the effects of fractional crystallization on the compositions of olivines must be evaluated to reveal the

mantle source of the Pohnpei Island OIBs.

Petrological modeling can help to elucidate the effects of fractional crystallization on magma compositions, but requires a primary magma composition as a starting point. To determine the primary magma composition as accurately as possible, the most common method is to correct the primitive melts or glasses assuming they have undergone fractionation only by crystallization of olivine (Herzberg et al., 2014). Zong et al. (2020) have calculated primary melt compositions using the method of Lee et al. (2009), and broadly reproduced the measured chemical composition of natural samples along liquid lines of descent (LLDs). However, the calculated primary melts consider only major elements rather than Ni, which is an important indicator in distinguishing peridotite versus pyroxenite mantle sources. In addition, Samples DS1 and DS2 contain abundant clinopyroxene phenocrysts, which complicates calculations estimating primary magma compositions. Therefore, we interpret our whole-rock and olivine data by comparing them with existing LLDs that assume a peridotite-source primary magma as the starting compositions.

Our whole-rock and olivine data plotted against modeled LLDs derived from a fertile peridotite and olivines crystallized therefrom (Herzberg, 2011) are shown in Figs 3 and 4. The fertile peridotite-derived primary magma is that produced in experiment 40.06 on Sample KR-4003 in the study of Walter (1998). The CaO, MnO, and Ni contents in Sample KR-4003 are 3.45 wt.%, 0.13 wt.%, and 1 964×$10^{-6}$, respectively. The whole-rock CaO, MnO, and Ni contents of the studied rocks are in good agreement with the modelled LLDs of primary magmas crystallizing olivine and then olivine + clinopyroxene + plagioclase (Figs 3a–c). This suggests that they share a common magmatic source. However, the chemical compositions of all of the Pohnpei olivines cannot be reproduced using the modeled olivine composition (Fig. 4). Most of the studied natural olivines have lower Ca contents than those from the primary (black field) and derivative (light blue field and black lines) magmas at a given Fo value. The low Ca contents in the Pohnpei olivines suggest advanced crystallization of considerable quantities of clinopyroxene, which will drive down the Ca contents of melts and olivines crystallized therefrom (Herzberg, 2011). The Ni and Mn contents of DS1 and DS2 olivine cores can be reproduced by the calculated olivines crystallized from derivative melts (8–20 wt.% MgO and 24–30 wt.% MgO; light blue fields and black lines). Rims of olivines in Sample DS1 have higher Ni and Mn contents than calculated LLDs olivines. Samples S7 and S8 contain olivines with higher Ni contents than calculated olivines, whereas their Mn contents match well will olivines modeled to have crystallized from derivative melts with 8–20 wt.% MgO.

### 5.2 *Mantle source lithology: peridotite or pyroxenite?*

The origin of the chemical and lithological heterogeneity (i.e., peridotite or pyroxenite) of the mantle source is one of the most important issues in understanding the petrogenesis of hotspot-related OIB (Sobolev et al., 2007; Herzberg et al., 2014; Elkins et al., 2019). The partial melts produced from pyroxenitic and peridotitic-mantle under similar *P*–*T* conditions have different major- and trace-element compositions, as do the olivines produced as these melts crystallize (Sobolev et al., 2005, 2007).

Only primitive melts inferred to have crystallized only olivine are generally selected to identify the mantle source of basalts (Le Roux et al., 2010; Yang and Zhou, 2013). Petrological modeling shows that the Pohnpei samples with >10 wt.% MgO might have mostly crystallized olivine (Fig. 3a). The CaO contents of the basalts with high MgO contents (>10 wt.%) fall within the peridotite melt field (Fig. 3a). The modeled LLDs also suggest that the studied Pohnpei basalts were derived from peridotite mantle (Figs 3a–c). In addition, whole-rock FeO/MnO ratios (Herzberg, 2011) and Zn/Fe ratios (Le Roux et al., 2010), along with FC3MS values ($FeO^T/CaO - (3 \times MgO/SiO_2)$; all in wt.%; Yang and Zhou, 2013), have been considered potential indicators for discriminating pyroxenite and peridotite mantle sources. The pyroxenite-derived melts were suggested to have high FeO/MnO ratios (>60; Herzberg, 2011), and 10 000×Zn/Fe ratios

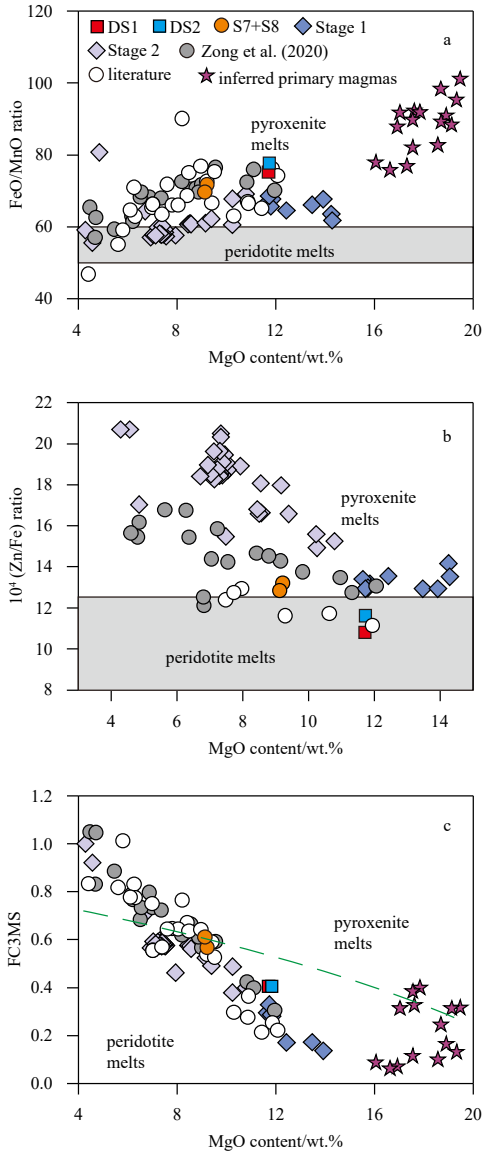


**Fig. 5.** FeO/MnO ratios (a), Zn/Fe ratios (b), and FC3MS ($FeO^T/CaO - (3 \times MgO/SiO_2)$) (c) ratios in olivines from the Pohnpei basalts. Literature data are from Mattey (1982), Dixon et al. (1984), and Jackson et al. (2017), and Stage 1 and Stage 2 basalts are from Zhang et al. (2020a). Inferred primary magmas for whole-rocks with >10 wt.% MgO were calculated using the model of Lee et al. (2009). The typical field for peridotite-derived melts compositions follows Herzberg (2011) in the diagram of FeO/MnO vs MgO, and Le Roux et al. (2010) in the diagram of Zn/Fe vs MgO. The boundary between peridotite-and pyroxenite-derived melts is based on the upper limit values of peridotite melts from Yang and Zhou (2013).

(>14; Le Roux et al., 2010) and FC3MS values (>0.65; Yang and Zhou, 2013), whereas peridotite-derived melts have low FeO/MnO ratios (50–60) and 10 000×Zn/Fe ratios (8.5–12.5) and FC3MS values (<0.65). The studied high-MgO basalts have FeO/MnO ratios of 60–80, and inferred primary magmas (Zong et al., 2020) with much higher FeO/MnO ratios (70 to 100; Fig. 5a). Samples DS1 and DS2 have lower Zn/Fe ratios (10.8 and 11.6, respectively), and most of the Pohnpei basalts have 10 000×Zn/Fe ratios ranging from 10 to 14 (Fig. 5b). Both indicators suggest that the Pohnpei samples were derived from a pyroxenite-dominated mantle source. However, FC3MS values range from 0.10 to ~0.65 for the high-MgO basalts and their inferred primitive magmas, which plot in the field of peridotite-derived melt. This finding is inconsistent with the FeO/MnO and Zn/Fe ratios in these samples.

The high-precision major- and trace-element compositions of olivine with high Fo have been widely used to identify the mantle sources of basalts (Sobolev et al., 2005, 2007). As olivines in Samples S7 and S8 and the rims of olivines in Sample DS1 have Fo values that are too low, we focus on olivines cores in Samples DS1 and DS2. Petrological modeling shows that with the exception of CaO, the chemical compositions of most olivines in Sample DS2 match well with the calculated LLDs of re-fertilized peridotite-derived magmas, but not with the olivines in Sample DS1 that have higher Fe/Mn ratios (Fig. 4). We compare the composition of olivine cores in Samples DS1 and DS2 with those from Mangaia Island in the Cook Islands (Fig. 4), which have similar Fo values to our data and are suggested to have originated from re-fertilized peridotite mantle (Herzberg et al., 2014). Olivines in Sample DS2 have similar Ni and Mn contents and Fe/Mn ratios to the Mangaia olivines. Thus, the former may be derived from re-fertilized peridotite mantle. In contrast, olivine cores in Sample DS1 have higher Fe/Mn values than the Mangaia olivines, but ratios that are similar to olivines from Hawaiian OIBs that have been interpreted as having originated from a pyroxenite mantle source (Herzberg, 2006; Sobolev et al., 2007). We use additional indicators, such as Ni/(Mg/Fe), Mn/Zn, and Zn/Fe ratios (Sobolev et al., 2007; Le Roux et al., 2010; Howarth and Harris, 2017), to identify the mantle source of the DS1 olivine cores. In order to draw a reliable conclusion, we chose olivine cores with high Fo (>80). As shown in Fig. 6, cores with high Fo have slightly higher Ni/(Mg/Fe) ratios than those from experimental peridotite-derived melts, and Mn/Zn ratios that fall in the field of pyroxenite-derived melts. However, these olivine cores have low Zn/Fe ratios, consistent with a peridotite mantle source.

The aforementioned geochemical indicators (Ni, Mn, Fe/Mn, Ni/(Mg/Fe), FC3MS, Mn/Zn, and Zn/Fe) may be used to discriminate the mantle source lithologies of basalts (Sobolev et al., 2007; Le Roux et al., 2010; Howarth and Harris, 2017), although there are some clear complications with respect to the Pohnpei samples. Studies have found that the Fe/Mn and Zn/Fe ratios in peridotite vary considerably (Le Roux et al., 2010). Partial melting of high Fe/Mn peridotite samples, such as KLB-1 (Hirose and Kushiro, 1993) and PHN1611 (Kushiro, 1996), should lead to high Fe/Mn ratios in the primary melt and olivines that crystallize therefrom. In addition, high *P*–*T* melting will decrease the parti-

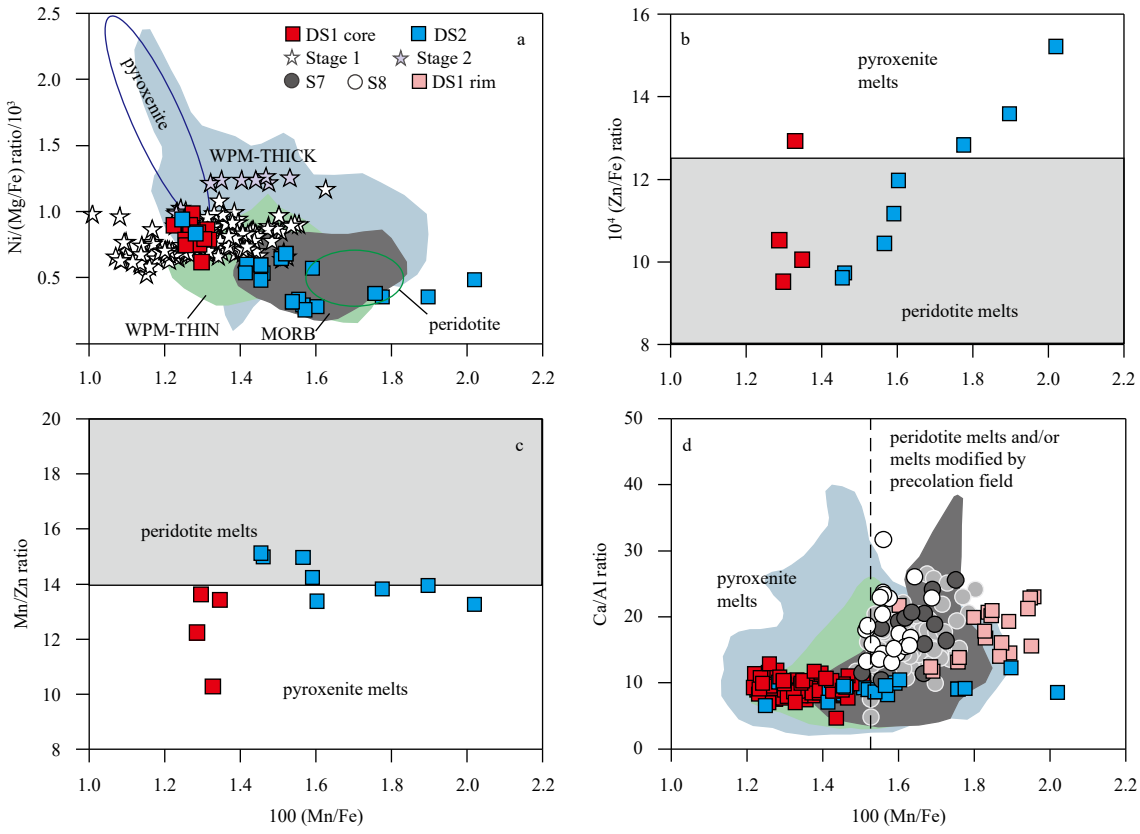


**Fig. 6.** 100 (Mn/Fe) vs Ni/(Mg/Fe) ratios/10³ (a), 10⁴ (Zn/Fe) ratios (b), Mn/Zn ratios (c), and Ca/Al ratios (d) in olivines from the Pohnpei basalts. Data for the Pohnpei olivines analyzed by Zong et al. (2020) and the Stage 1 and Stage 2 olivines reported by Zhang et al. (2020a) are also shown. Olivine data from MORB, the WPM-THIN and WPM-THICK basalts, and the fields for olivine crystallized from pyroxenite- and peridotite-derived melts are from Sobolev et al. (2007).

tion coefficient for Ni, but increase the partition coefficient for Mn and Mn/Fe ratio between olivine and liquid (Li and Ripley, 2010; Niu et al., 2011; Matzen et al., 2013, 2017b), thereby increasing Ni concentrations and decreasing Mn contents and Mn/Fe and Mn/Zn ratios in melt and olivine crystallized therefrom (Putirka et al., 2018). Recent studies have shown that the Pohnpei lavas were produced at high mantle pressures (average (3.8 ± 0.7) GPa) and temperatures (average (1 557 ± 43)°C) (Zong et al., 2020), which may account for the apparent "pyroxenite signal" preserved in the cores of olivine grains in Sample DS1.

### 5.3 *Implications for the magmatic evolution*

In Sample DS1, almost all olivines show clear normal zonation with more primitive (higher Fo) cores that are surrounded by more evolved rims. The abrupt change in chemical compositions between cores and rims indicates that magma recharge and mixing occurred (De Maisonneuve et al., 2016; Gleeson and Gibson, 2019). Cores and rims of olivines in Sample DS1 did not form by fractional crystallization of a primary magma, and the compositions of the cores are not in equilibrium with their host whole-rock, suggesting the cores may be antecrysts that crystallized from an earlier batch of magma that then underwent magma recharge and mixing, and were entrained in the magma in which they are now hosted (Larrea et al., 2013). The normal compositional zonation implies that the cores originated through magma recharge that interacted with cooler crystals prior to eruption (De Maisonneuve et al., 2016). This magma mixing event is supported by the presence of clinopyroxenes that also preserve chemical zonation (Figs 2k and l in Zong et al. (2020)).

Olivine cores in Sample DS1 have constant Fe/Mn ratios, and their Mn and Ni contents correlate strongly with Fo values (Figs 4b–d), suggesting fractional crystallization of a cogenetic primary magma. The constant Ca contents at variable Fo values indicate that the primary magma might have undergone co-crystallization of olivine and clinopyroxene (Herzberg et al., 2014; Gleeson and Gibson, 2019), consistent with the petrographic observations that indicate these basalts contain a large quantity of olivine and clinopyroxene. Olivine rims in Sample DS1 have different Ca, Ni, and Mn contents and Fe/Mn ratios than cores, indicating that the replenished magma was not cognate with the host magma of the cores. The increase in Ca contents with decreasing Fo indicates that the mixed magma might have undergone an evolution dominated by olivine crystallization. Olivine Ca/Al ratios can be used to estimate the crystallization temperature of olivine, with high Ca/Al ratios reflecting lower temperature (De Hoog et al., 2010; Coogan et al., 2014; Gómez-Ulla et al., 2017). As shown in Fig. 6, olivine cores from Sample DS1 have lower Ca/Al ratios than rims, indicating that the cores were formed at higher temperature (or greater depth). Accordingly, we suggest that the magma that crystallized the olivine cores formed under high pressures and temperatures in a deep magma chamber. This magma migrated upward into a shallower magma chamber and mixed with a preexisting melt, then continued to crystallize to form the olivine rims.

Olivine grains in Sample DS2 have higher Mn/Fe ratios but similar Ca/Al ratios relative to cores (Fig. 6), implying that their host magmas might not have been cognate, but crystallized under similar *P*–*T* conditions. Olivines in Samples S7 and S8 have similar chemical compositions to olivine rims in Sample DS1, indicating that their host magmas might have been cogenetic.

## 6 Conclusions

We undertook an integrated study combining whole-rock and *in-situ* olivine compositions in basaltic lavas from the Pohnpei Island. We draw the following conclusions regarding the source and evolution of the magmas:

(1) The olivine phenocrysts show large systematic inter- and intra-crystalline compositional variations, suggesting a strong influence from fractional crystallization. Olivine cores in Samples DS1 and DS2 formed at greater depth than olivines in Samples S7 and S8. Olivines in Sample DS1 preserve compositional zonation, indicating that their host magmas experienced magma recharge and mixing. The host magmas of olivine cores in Sample DS1 might have undergone co-crystallization of olivine and clinopyroxene in a deep magma chamber, then carried olivines cores upward into a shallower magma chamber where they recharged and mixed with a preexisting melt, leading to the formation of olivine rims with lower Fo.

(2) Forward petrological modeling and multi-element indicators yield contradictory results as discriminators of the mantle source (i.e., pyroxenite mantle vs peridotite mantle). For example, Fe/Mn and Ni/(Mg/Fe) ratios in DS1 olivine cores are consistent with a pyroxenite mantle source, whereas Zn/Fe ratios (<12) suggest a peridotite mantle source. These conflicting results may indicate that partial melting and the subsequent evolution of the magma affected the olivine compositions. We suggest that the identification of the mantle source of basalts by means of olivine geochemistry should be treated with caution.

### *Acknowledgements*

We appreciate the help of Xiaohong Wang with the Institute of Oceanology, Chinese Academy of Sciences, for LA-ICP-MS analysis.

## References

Ammannati E, Jacob D E, Avanzinelli R, et al. 2016. Low Ni olivine in silica-undersaturated ultrapotassic igneous rocks as evidence for carbonate metasomatism in the mantle. Earth and Planetary Science Letters, 444: 64–74, doi: 10.1016/j.epsl.2016.03.039

Collinet M, Charlier B, Namur O, et al. 2017. Crystallization history of enriched shergottites from Fe and Mg isotope fractionation in olivine megacrysts. Geochimica Et Cosmochimica Acta, 207: 277–297, doi: 10.1016/j.gca.2017.03.029

Coogan L A, Saunders A D, Wilson R N. 2014. Aluminum-in-olivine thermometry of primitive basalts: Evidence of an anomalously hot mantle source for large igneous provinces. Chemical Geology, 368: 1–10, doi: 10.1016/j.chemgeo.2014.01.004

Courtillot V, Davaille A, Besse J, et al. 2003. Three distinct types of hotspots in the Earth's mantle. Earth and Planetary Science Letters, 205(3–4): 295–308, doi: 10.1016/S0012-821X(02)01048-8

De Hoog J C M, Gall L, Cornell D H. 2010. Trace-element geochemistry of mantle olivine and application to mantle petrogenesis and geothermobarometry. Chemical Geology, 270(1–4): 196–215, doi: 10.1016/j.chemgeo.2009.11.017

De Maisonneuve C B, Costa F, Huber C, et al. 2016. How do olivines record magmatic events? Insights from major and trace element zoning. Contributions to Mineralogy and Petrology, 171(6): 56, doi: 10.1007/s00410-016-1264-6

Dixon T H, Batiza R, Futa K, et al. 1984. Petrochemistry, age and isotopic composition of alkali basalts from Ponape Island, western Pacific. Chemical Geology, 43(1–2): 1–28, doi: 10.1016/0009-2541(84)90138-4

Elkins L J, Bourdon B, Lambart S. 2019. Testing pyroxenite versus peridotite sources for marine basalts using U-series isotopes. Lithos, 332–333: 226–244, doi: 10.1016/j.lithos.2019.02.011

Foley S F, Prelevic D, Rehfeldt T, et al. 2013. Minor and trace elements in olivines as probes into early igneous and mantle melting processes. Earth and Planetary Science Letters, 363: 181–191, doi: 10.1016/j.epsl.2012.11.025

Gleeson M L M, Gibson S A. 2019. Crustal controls on apparent

mantle pyroxenite signals in ocean-island basalts. Geology, 47(4): 321–324, doi: 10.1130/G45759.1

Gómez-Ulla A, Sigmarsson O, Gudfinnsson G H. 2017. Trace element systematics of olivine from historical eruptions of Lanzarote, Canary Islands: Constraints on mantle source and melting mode. Chemical Geology, 449: 99–111, doi: 10.1016/j.chemgeo.2016.11.021

Heinonen J S, Fusswinkel T. 2017. High Ni and low Mn/Fe in olivine phenocrysts of the Karoo meimechites do not reflect pyroxenitic mantle sources. Chemical Geology, 467: 134–142, doi: 10.1016/j.chemgeo.2017.08.002

Herzberg C. 2006. Petrology and thermal structure of the Hawaiian plume from Mauna Kea volcano. Nature, 444(7119): 605–609, doi: 10.1038/nature05254

Herzberg C. 2011. Identification of source lithology in the Hawaiian and Canary Islands: Implications for origins. Journal of Petrology, 52(1): 113–146, doi: 10.1093/petrology/egq075

Herzberg C, Asimow P D. 2008. Petrology of some oceanic island basalts: PRIMELT2. XLS software for primary magma calculation. Geochemistry, Geophysics, Geosystems, 9(9): Q09001, doi: 10.1029/2008GC002057

Herzberg C, Asimow P D, Ionov D A, et al. 2013. Nickel and helium evidence for melt above the core–mantle boundary. Nature, 493(7432): 393–397, doi: 10.1038/nature11771

Herzberg C, Cabral R A, Jackson M G, et al. 2014. Phantom Archean crust in Mangaia hotspot lavas and the meaning of heterogeneous mantle. Earth and Planetary Science Letters, 396: 97–106, doi: 10.1016/j.epsl.2014.03.065

Herzberg C, Vidito C, Starkey N A. 2016. Nickel-cobalt contents of olivine record origins of mantle peridotite and related rocks. American Mineralogist, 101(9): 1952–1966, doi: 10.2138/am-2016-5538

Hirose K, Kushiro I. 1993. Partial melting of dry peridotites at high pressures: Determination of compositions of melts segregated from peridotite using aggregates of diamond. Earth and Planetary Science Letters, 114(4): 477–489, doi: 10.1016/0012-821X(93)90077-M

Hofmann A W, White W M. 1982. Mantle plumes from ancient oceanic crust. Earth and Planetary Science Letters, 57(2): 421–436, doi: 10.1016/0012-821X(82)90161-3

Howarth G H, Harris C. 2017. Discriminating between pyroxenite and peridotite sources for continental flood basalts (CFB) in southern Africa using olivine chemistry. Earth and Planetary Science Letters, 475: 143–151, doi: 10.1016/j.epsl.2017.07.043

Huang Shichun, Zheng Yongfei. 2017. Mantle geochemistry: Insights from ocean island basalts. Science China Earth Sciences, 60(11): 1976–2000, doi: 10.1007/s11430-017-9090-4

Jackson M G, Price A A, Blichert-Toft J, et al. 2017. Geochemistry of lavas from the Caroline hotspot, Micronesia: Evidence for primitive and recycled components in the mantle sources of lavas with moderately elevated $^{3}He/^{4}He$. Chemical Geology, 455: 385–400, doi: 10.1016/j.chemgeo.2016.10.038

Keating B H, Mattey D P, Helsley C E, et al. 1984. Evidence for a hot spot origin of the Caroline Islands. Journal of Geophysical Research: Solid Earth, 89(B12): 9937–9948, doi: 10.1029/JB089iB12p09937

Kushiro I. 1996. Partial melting of a fertile mantle peridotite at high pressures: An experimental study using aggregates of diamond. In: Basu A, Hart S, eds. Earth Processes: Reading the Isotopic Code. Geophysical Monograph Series. Washington, DC: American Geophysical Union, 95: 109–122, doi: 10.1029/GM095p0109

Larrea P, França Z, Lago M, et al. 2013. Magmatic processes and the role of antecrysts in the genesis of Corvo Island (Azores Archipelago, Portugal). Journal of Petrology, 54(4): 769–793, doi: 10.1093/petrology/egs084

Le Roux V, Lee C T A, Turner S J. 2010. Zn/Fe systematics in mafic and ultramafic systems: Implications for detecting major element heterogeneities in the Earth's mantle. Geochimica Et Cosmochimica Acta, 74(9): 2779–2796, doi: 10.1016/j.gca.2010.02.004

Lee C T A, Luffi P, Plank T, et al. 2009. Constraints on the depths and temperatures of basaltic magma generation on Earth and other terrestrial planets using new thermobarometers for mafic magmas. Earth and Planetary Science Letters, 279(1–2): 20–33, doi: 10.1016/j.epsl.2008.12.020

Li C S, Ripley E M. 2010. The relative effects of composition and temperature on olivine-liquid Ni partitioning: Statistical deconvolution and implications for petrologic modeling. Chemical Geology, 275(1–2): 99–104, doi: 10.1016/j.chemgeo.2010.05.001

Li Xiaohui, Zeng Zhigang, Dan Wei, et al. 2020. Source lithology and crustal assimilation recorded in low $\delta^{18}O$ olivine from Okinawa Trough, back-arc basin. Lithos, 360–361: 105444, doi: 10.1016/j.lithos.2020.105444

Lissenberg C J, MacLeod C J. 2016. A reactive porous flow control on mid-ocean ridge magmatic evolution. Journal of Petrology, 57(11–12): 2195–2220, doi: 10.1093/petrology/egw074

Liu Yongsheng, Hu Zhaochu, Gao Shan, et al. 2008. *In situ* analysis of major and trace elements of anhydrous minerals by LA-ICP-MS without applying an internal standard. Chemical Geology, 257(1–2): 34–43, doi: 10.1016/j.chemgeo.2008.08.004

Mattey D P. 1982. The minor and trace element geochemistry of volcanic rocks from Truk, Ponape and Kusaie, eastern Caroline Islands; the evolution of a young hot spot trace across old Pacific Ocean crust. Contributions to Mineralogy and Petrology, 80(1): 1–13, doi: 10.1007/BF00376730

Matzen A K, Baker M B, Beckett J R, et al. 2013. The temperature and pressure dependence of nickel partitioning between olivine and silicate melt. Journal of Petrology, 54(12): 2521–2545, doi: 10.1093/petrology/egt055

Matzen A K, Baker M B, Beckett J R, et al. 2017b. The effect of liquid composition on the partitioning of Ni between olivine and silicate melt. Contributions to Mineralogy and Petrology, 172(1): 3, doi: 10.1007/s00410-016-1319-8

Matzen A K, Wood B J, Baker M B, et al. 2017a. The roles of pyroxenite and peridotite in the mantle sources of oceanic basalts. Nature Geoscience, 10(7): 530–535, doi: 10.1038/ngeo2968

McDonough W F, Sun S S. 1995. The composition of the Earth. Chemical Geology, 120(3–4): 223–253, doi: 10.1016/0009-2541(94)00140-4

Morgan W J. 1971. Convection plumes in the lower mantle. Nature, 230(5288): 42–43, doi: 10.1038/230042a0

Niu Yaoling, Wilson M, Humphreys E R, et al. 2011. The origin of intra-plate ocean island basalts (OIB): The lid effect and its geodynamic implications. Journal of Petrology, 52(7–8): 1443–1468, doi: 10.1093/petrology/egr030

O'Neill H S C, Jenner F E. 2016. Causes of the compositional variability among ocean floor basalts. Journal of Petrology, 57(11–12): 2163–2194, doi: 10.1093/petrology/egx001

Paquet M, Cannat M, Brunelli D, et al. 2016. Effect of melt/mantle interactions on MORB chemistry at the easternmost Southwest Indian Ridge (61°–67°E). Geochemistry, Geophysics, Geosystems, 17(11): 4605–4640, doi: 10.1002/2016GC006385

Putirka K D. 2008. Introduction to minerals, inclusions and volcanic processes. Reviews in Mineralogy and Geochemistry, 69(1): 1–8, doi: 10.2138/rmg.2008.69.1

Putirka K, Tao Y, Hari K R, et al. 2018. The mantle source of thermal plumes: Trace and minor elements in olivine and major oxides of primitive liquids (and why the olivine compositions don't matter). American Mineralogist, 103(8): 1253–1270, doi: 10.2138/am-2018-6192

Rehkämper M, Hofmann A W. 1997. Recycled ocean crust and sediment in Indian Ocean MORB. Earth and Planetary Science Letters, 147(1–4): 93–106, doi: 10.1016/S0012-821X(97)00009-5

Rehman H U, Nakaya H, Kawai K. 2013. Geological origin of the volcanic islands of the Caroline group in the Federated States of Micronesia, western Pacific. South Pacific Studies, 33(2): 101–118

Ren Zhongyuan, Takahashi E, Orihashi Y, et al. 2004. Petrogenesis of tholeiitic lavas from the submarine Hana ridge, Haleakala volcano, Hawaii. Journal of Petrology, 45(10): 2067–2099, doi: 10.1093/petrology/egh076

Shaikh A M, Patel S C, Bussweiler Y, et al. 2019. Olivine trace element compositions in diamondiferous lamproites from India: Proxies for magma origins and the nature of the lithospheric mantle beneath the Bastar and Dharwar cratons. Lithos, 324–325: 501–518, doi: 10.1016/j.lithos.2018.11.026

Shorttle O. 2015. Geochemical variability in MORB controlled by concurrent mixing and crystallisation. Earth and Planetary Science Letters, 424: 1–14, doi: 10.1016/j.epsl.2015.04.035

Sobolev A V, Hofmann A W, Kuzmin D V, et al. 2007. The amount of recycled crust in sources of mantle-derived melts. Science, 316(5823): 412–417

Sobolev A V, Hofmann A W, Sobolev S V, et al. 2005. An olivine-free mantle source of Hawaiian shield basalts. Nature, 434(7033): 590–597, doi: 10.1038/nature03411

Spengler S R. 1990. Geology and hydrogeology of the island of Pohnpei, Federated States of Micronesia [dissertation]. Honolulu, HI: University of Hawaii at Manoa

Spengler S, Spencer K, Mahoney J G G. 1994. Geology and geochemical evolution of lavas on the island of Pohnpei, Federated States of Micronesia. http://e2hi.s3.amazonaws.com/element-environmental-llc/uploads/attachment/attachment/32/12_Geology_and_Geochemical_Evolution_of_Lavas_on_the_Island_of_Pohnpei.pdf [2021-01-01]/[2021-04-20]

Stracke A. 2012. Earth's heterogeneous mantle: A product of convection-driven interaction between crust and mantle. Chemical Geology, 330–331: 274–299, doi: 10.1016/j.chemgeo.2012.08.007

Sun S S, McDonough W F. 1989. Chemical and isotopic systematics of oceanic basalts: Implications for mantle composition and processes. Geological Society London Special Publications, 42(1): 313–345, doi: 10.1144/gsl.sp.1989.042.01.19

Thompson R N, Gibson S A. 2000. Transient high temperatures in mantle plume heads inferred from magnesian olivines in Phanerozoic picrites. Nature, 407(6803): 502–506, doi: 10.1038/35035058

Vidito C, Herzberg C, Gazel E, et al. 2013. Lithological structure of the Galápagos plume. Geochemistry, Geophysics, Geosystems, 14(10): 4214–4240, doi: 10.1002/ggge.20270

Walter M J. 1998. Melting of garnet peridotite and the origin of komatiite and depleted lithosphere. Journal of Petrology, 39(1): 29–60, doi: 10.1093/petroj/39.1.29

Wang Xuance, Li Zhengxiang, Li Xianhua, et al. 2012. Temperature, pressure, and composition of the mantle source region of late Cenozoic basalts in Hainan Island, SE Asia: A consequence of a young thermal mantle plume close to subduction zones?. Journal of Petrology, 53(1): 177–233, doi: 10.1093/petrology/egr061

Yang Zongfeng, Zhou Junhong. 2013. Can we identify source lithology of basalt?. Scientific Reports, 3(1): 1856, doi: 10.1038/srep01856

Yaxley G M. 2000. Experimental study of the phase and melting relations of homogeneous basalt + peridotite mixtures and implications for the petrogenesis of flood basalts. Contributions to Mineralogy and Petrology, 139(3): 326–338, doi: 10.1007/s004100000134

Yaxley G M, Green D H. 1998. Reactions between eclogite and peridotite: Mantle refertilisation by subduction of oceanic crust. Schweizerische Mineralogische und Petrographische Mitteilungen, 78(2): 243–255

Zamboni D, Trela J, Gazel E, et al. 2017. New insights into the Aeolian Islands and other arc source compositions from high-precision olivine chemistry. Lithos, 272–273: 185–191, doi: 10.1016/j.lithos.2016.12.004

Zhang Guoliang, Wang Shuai, Zhang Ji, et al. 2020a. Evidence for the essential role of $CO_2$ in the volcanism of the waning Caroline mantle plume. Geochimica et Cosmochimica Acta, 290: 391–407, doi: 10.1016/j.gca.2020.09.018

Zhang Guoliang, Zhang Ji, Wang Shuai, et al. 2020b. Geochemical and chronological constraints on the mantle plume origin of the Caroline Plateau. Chemical Geology, 540: 119566, doi: 10.1016/j.chemgeo.2020.119566

Zong Tong, Li Zhenggang, Dong Yanhui, et al. 2020. Geochemical constraints on mantle melting and magma genesis at Pohnpei island, Micronesia. Minerals, 10(9): 816, doi: 10.3390/min10090816

## Supplementary information:

**Table S1**. Results of whole-rock major (wt.%) and trace element ($10^{-6}$) compositions for the DS1 and DS2 samples from the Pohnpei Island.

**Table S2**. Results of *in situ* EPMA major element (wt.%) analyses of olivines in the basalts from the Pohnpei Island.

**Table S3**. Results of *in situ* LA-ICP-MS major and trace element analyses of olivines in the basalts from the Pohnpei Island.

**Table S4**. Results of *in situ* LA-ICP-MS major and trace element analyses and the recommended reference value of the standards GSE-1G, BCR-2G, BHVO-2G, and BIR-1G glasses.

The supplementary information is available online at https://doi.org/10.1007/s13131-021-1901-4 and http://www.aosocean.com/. The supplementary information is published as submitted, without typesetting or editing. The responsibility for scientific accuracy and content remains entirely with the authors.

# Appendix:

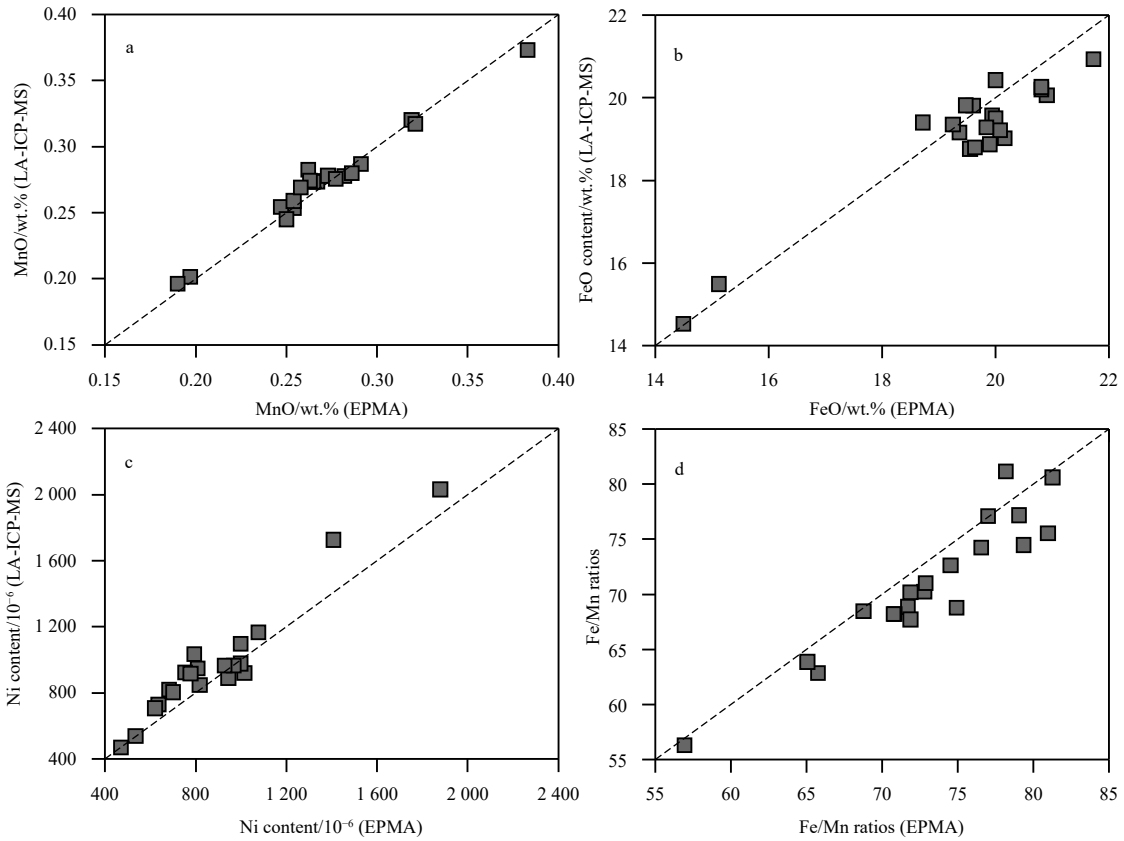


**Fig. A1.** Comparison of MnO (a), FeO (b), Ni (c) contents and Fe/Mn ratios (d) in the analyzed olivines obtained by LA-ICP-MS and EPMA, respectively.

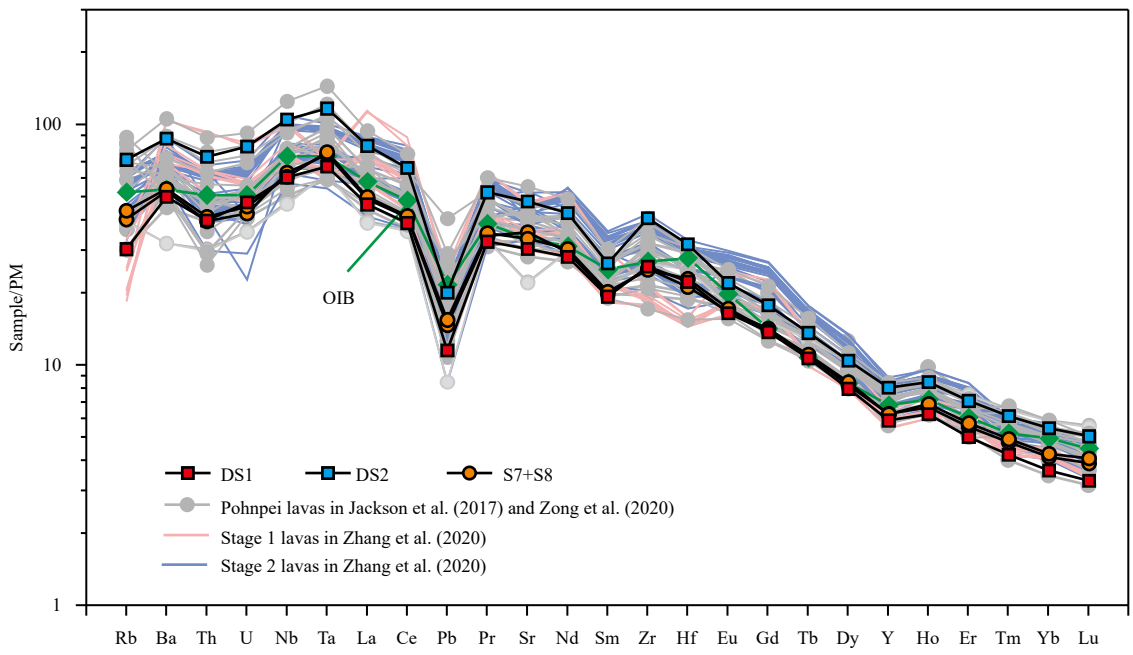


**Fig. A2.** Primitive mantle (PM; McDonough and Sun, 1995)-normalized trace element patterns of Pohnpei lavas. OIBs (ocean island basalts) trace element data are from Sun and McDonough (1989).

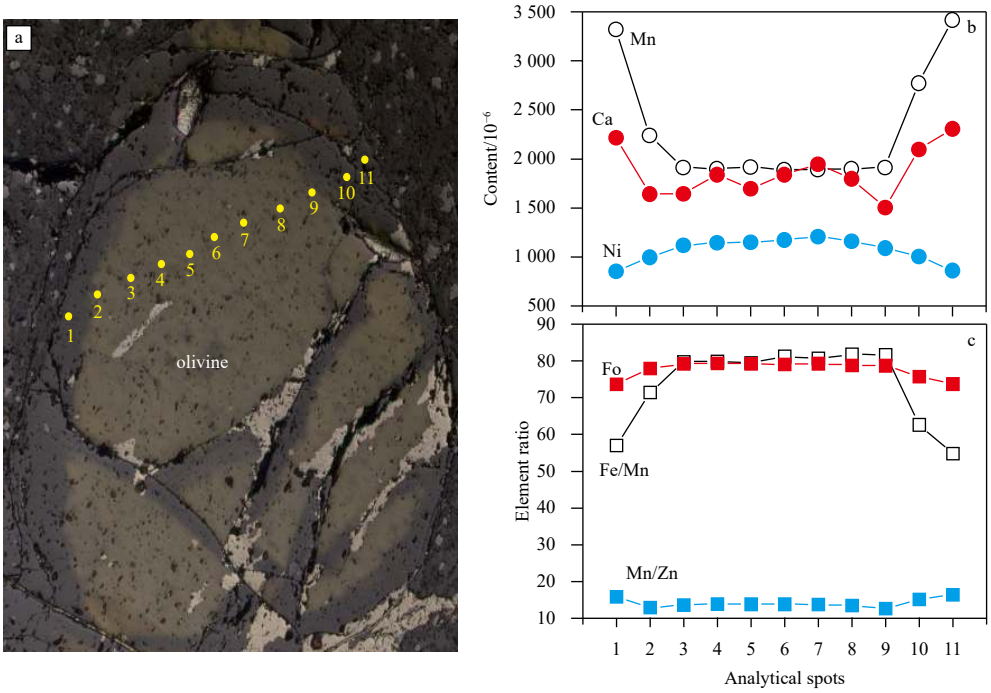


**Fig. A3.** Representative photomicrographs and analytical points with chemical compositions for representative olivine crystal in DS1. The yellow points were the analytical spots by electron probe microanalyser (EPMA).

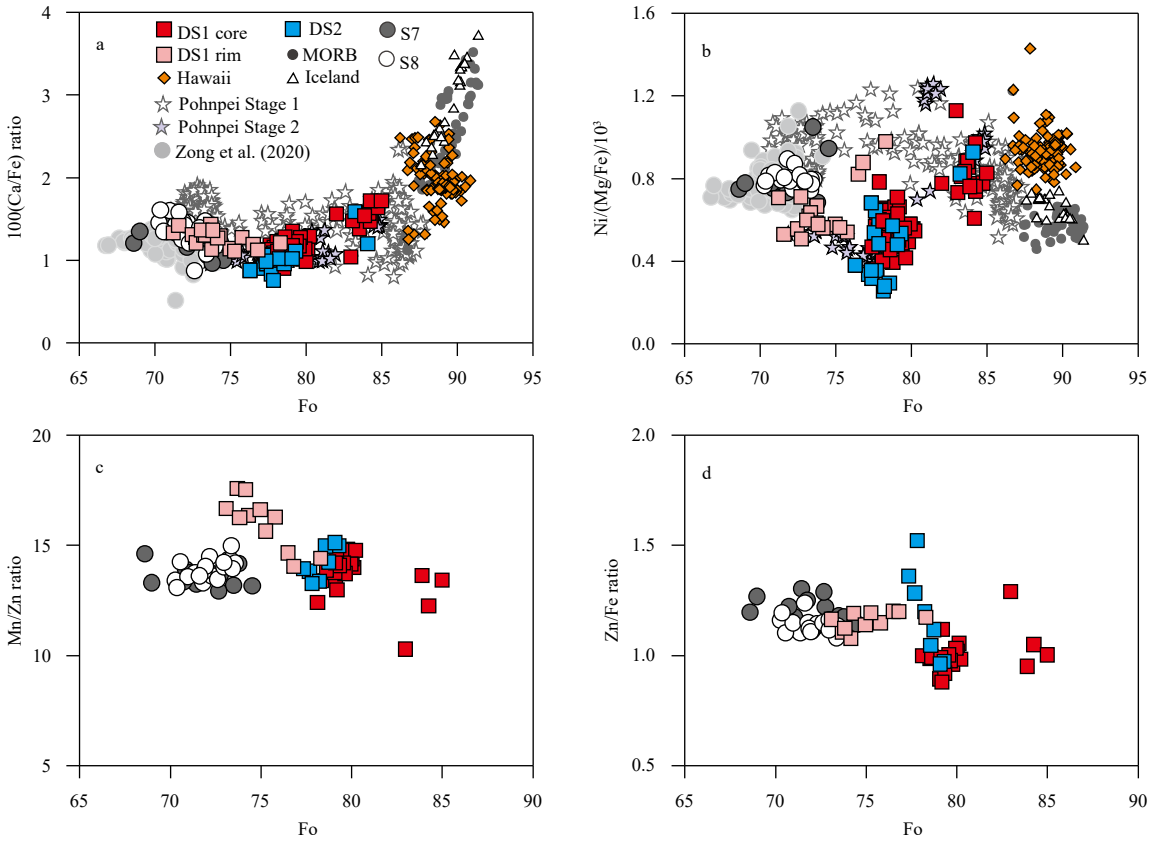


**Fig. A4.** The representative trace elements ratios against Fo values of the olivines from Pohnpei basalts. The data of Pohnpei olivines analyzed by Zong et al. (2020) and Pohnpei Stage 1 and Stage 2 basalts reported by Zhang et al. (2020a) are also plotted. The data of olivines in MORBs, Hawaii and Iceland basalts are from Sobolev et al. (2007).